Journal of Advances in Physical Chemistry 物理化学进展, 2024, 13(4), 795-809
Published Online November 2024 in Hans. https://www.hanspub.org/journal/japc
https://doi.org/10.12677/japc.2024.134079

Hans汉斯

锌－稀土单分子磁体的研究进展

胡翔宇[1]，梁皓然[1]，徐嘉琦[1]，解梦婷[1]，王窦尊[1]，郑　祺[1]，崔会会[1,2*]

[1]南通大学化学化工学院，江苏　南通
[2]南通市智能与新能源材料及器件重点实验室，江苏　南通

收稿日期：2024年10月16日；录用日期：2024年11月21日；发布日期：2024年11月29日

摘　要

锌(II) d轨道的电子是全充满的，它通过与配体形成配位键。在结构中提供金属骨架，并通过桥联配体与稀土元素连接，间接影响稀土离子的磁性行为。近年来，锌－稀土金属配合物在分子磁性材料领域受到广泛关注，因此，本文通过对近年来典型的锌－稀土单分子磁体进行综述，以期为3d-4f单分子磁体的发展奠定一定的基础。

关键词

锌－稀土单分子磁体，结构，磁性

Research Progress in Zn-Ln Single Molecule Magnets

Xiangyu Hu[1], Haoran Liang[1], Jiaqi Xu[1], Mengting Xie[1], Douzun Wang[1], Qi Zheng[1], Huihui Cui[1,2*]

[1]School of Chemistry and Chemical Engineering, Nantong University, Nantong Jiangsu
[2]Nantong Key Laboratory of Intelligent and New Energy Materials and Devices, Nantong Jiangsu

Received: Oct. 16th, 2024; accepted: Nov. 21st, 2024; published: Nov. 29th, 2024

Abstract

The electrons of the zinc(II) d orbital are fully filled, which can form coordination bonds with ligands. It provides a metal skeleton in the structure and is connected to lanthanide elements by bridging ligands, indirectly affecting the magnetic behavior of lanthanide ions. In recent years, zinc-lanthanide metal complexes have received extensive attention in the field of molecular magnetic materials.

*通讯作者。

文章引用: 胡翔宇, 梁皓然, 徐嘉琦, 解梦婷, 王窦尊, 郑祺, 崔会会. 锌-稀土单分子磁体的研究进展[J]. 物理化学进展, 2024, 13(4): 795-809. DOI: 10.12677/japc.2024.134079

Therefore, this paper reviews the typical zinc-lanthanide single molecule magnets (SMMs) in recent years, hoping to lay a certain foundation for the development of 3d-4f SMMs.

Keywords

Zn-Ln Single Molecule Magnets, Structure, Magnetism

1. 引言

在过去的十几年里，关于 f 元素的配合物发表数量呈指数级增长，这些化合物大多都显示出磁矩的缓慢弛豫。由于强烈的自旋－轨道耦合和晶体场效应[1]-[3]，稀土离子具有显著的单离子各向异性，大的总角矩(J)使其成为 SMM 的优良自旋载流子。然而，由于 4f 轨道的有限径向伸展展现出了非常弱，甚至没有交换作用的现象。而其中一种提供强磁交换相互作用的方法是将 3d 离子引入 4f 系统，并且分子的大基态和磁各向异性可以通过控制磁交换相互作用力来引导。通过增加配合物中 3d 和 4f 离子之间的磁耦合，利用 4f 离子的单离子各向异性来增加 U_{eff}。

锌作为一种过渡金属，通常是没有未配对电子，所以其本身不具备磁性。其主要作用是通过与稀土金属的相互反应作用，改变分子结构和改变配位稀土的局部环境，影响稀土金属的磁性行为。因其在 4f 轨道的特殊结构，表现出高磁矩和磁各向异性。这类化合物的潜在应用包括信息存储、量子计算、磁制冷等领域[4]-[6]。

Zn-Ln 单分子磁体是一类具有特殊磁性和光学性能的配合物。这类配合物一般通过锌和稀土元素的相互作用形成。其结构多样且具有独特的拓扑结构。近年来，锌－稀土金属配合物在分子磁性材料领域受到广泛关注，并表现出独特潜力。因此，构建 Zn-Ln SMMs 受到了科学家们的广泛关注。

2. 锌－稀土单分子磁体的研究进展

目前，已报道的锌－稀土单分子磁体如表 1 所示，本论文仅选取其中一些例子进行描述，并根据其核数进行分类，以研究其结构与磁性之间的关系。

Table 1. The magnetic data of Zn-Ln SMMs
表 1. Zn-Ln 单分子磁体的磁性数据

Complexes	H_{dc}/kOe	U_{eff}/K	τ_0/s	v/mT/s	T_B/K	Ref.
$[Zn_2Dy(L^1)_2(MeOH)]\cdot NO_3\cdot 3MeOH\cdot H_2O$ (**1**)	0	439		20	11	[1]
$[Zn_2Dy(L^1)_2]NO_3\cdot H_2O$ (**2**)	1.2	64				[1]
$[ZnCl(\mu\text{-}L^2)Dy(\mu\text{-}L^2)ClZn][ZnCl_3(CH_3OH)]\cdot 3CH_3OH$ (**3**)	1	24.3	$1.07(3)\times 10^{-7}$			[2]
$[(L^3Zn(H_2O))_2Dy(H_2O)](CF_3SO_3)_3$ (**4**)	0	96.9 (6)	2.4×10^{-7}			[3]
$[(L^3ZnBr)_2Dy(H_2O)](ClO_4)$ (**5**)	1	214.7	9.8×10^{-9}			[3]
$[(L^3ZnCl)_2Dy(H_2O)](ClO_4)(MeOH)$ (**6**)	1	202.4	1.5×10^{-8}			[3]
$[Zn_2(L^4)_2DyCl_3]\cdot 2H_2O$ (**7**)	0	430	7.4×10^{-11}	20	12	[4]
$[Zn_2(L^4)_2Dy(MeOH)Br_3]\cdot 3H_2O$ (**8**)	0	233	2.5×10^{-8}		6	[4]

续表

$[Zn_2(L^4)_2Dy(H_2O)Br_2]\cdot[ZnBr_4]_{0.5}$ (**9**)	0	121	8.5×10^{-7}		4	[4]
$[Zn_2(L^5)_2DyCl_3]\cdot2H_2O$ (**10**)	0	398	3.5×10^{-10}		8	[4]
$[Zn_2Dy(TTTTCl)_2Me_2CO]\cdot NO_3\cdot EtOH\cdot H_2O$ (**11**)	0	507 (7)	$2.0\ (5)\times10^{-11}$	20	14	[5]
$[Zn_2Dy(TTTTCl)_2MeOH]\cdot CF_3SO_3\cdot2MeOH$ (**12**)	0	525 (6)	$1.0\ (2)\times10^{-11}$	20	12	[5]
$[Zn_2Dy(TTTTCl)_2Me_2CO]\cdot BPh_4\cdot3Me_2CO\cdot EtOH\cdot4H_2O$ (**13**)	0	632 (2)	$3.4\ (1)\times10^{-12}$	20	23	[5]
$[Zn_2Dy(TTTTCl)_2DMF]\cdot BPh_4\cdot2THF\cdot EtOH\cdot0.5DMF\cdot2H_2O$ (**14**)	0	535 (2)	$2.4\ (1)\times10^{-11}$	20	22	[5]
$[Zn_2Dy(TTTTCl)_2NMP]\cdot BPh_4\cdot3THF\cdot2H_2O$ (**15**)	0	558 (3)	$1.5\ (1)\times10^{-11}$	20	24	[5]
$[ZnDy(L^6)(DBM)_3]$ (**16**)	2	36.5	1.56×10^{-6}			[6]
$[ZnDy(H_4L^7)_2](NO_3)_3\cdot6H_2O$ (**17**)	0	270.3	2.67×10^{-10}	5	2	[7]
$[Dy_2Zn_2(L^5)_4(NO_3)_2(CH_3OH)_2]$ (**18**)	0	78	4.59×10^{-6}		4	[8]
$[Zn_2Dy_2(L^8)_4(NO_3)_2(CH_3OH)_2]\cdot2CH_3COCH_3$ (**19**)	0	111.5	8.2×10^{-5}			[9]
$[Zn_2Dy_2(L^8)_4(CH_3COO)_2(CH_3CH_2OH)_2]\cdot4CH_3COCH_3$ (**20**)	0	74.4	2.78×10^{-6}			[9]
$[Zn_2(L^9)_2(PhCOO)_2Dy_2(hfac)_4]$ (**21**)	0	47.9	2.75×10^{-7}			[10]
$[Dy_6Zn_4O_2(L^{10})_2(HL^{10})_2(OAc)_8(CH_3O)_4(H_2O)_2]\cdot4MeOH$ (**22**)	0	43	1×10^{-5}			[11]
$[Zn_3Dy_3(O_2)(L^{11})_3(PyCO_2)_3](OH)_2(ClO_4)_2\cdot8H_2O$ (**23**)	1	100.4 (3.9)	$1.2\ (0.4)\times10^{-8}$			[12]
$[Zn_3Tb_3(O_2)(L^{11})_3(PyCO_2)_3](OH)_2(ClO_4)_2\cdot8H_2O$	1.4	14.4 (0.5)	$4.3\ (0.2)\times10^{-6}$			[13]
$[Zn_2Dy_3(m\text{-salen})_3(N_3)_5(OH)_2]$	0	13.40	3.3×10^{-7}	17	1.1	[13]
$[Zn_3Dy(L^{Pr})(NO_3)_3(MeOH)_3]\cdot4H_2O$	1.5	25.8	1.2×10^{-6}			[14]
$[Tb\{Zn(L^{12})(AcO)\}_2]BPh_4$	1	35 (1)	$1.6\ (2)\times10^{-6}$			[15]
$[Dy\{Zn(L^{12})(AcO)\}_2]BPh_4$	1	22.4 (4)	$5.3\ (4)\times10^{-7}$			[15]
$[Er\{Zn(L^{12})(AcO)\}_2]BPh_4$	1	42 (3)	$9\ (6)\times10^{-10}$			[15]
$[Yb\{Zn(L^{12})(AcO)\}_2]BPh_4$	1	38.2 (4)	$7.0\ (5)\times10^{-8}$			[15]
$[Zn_2Dy_2(hmp)_4(PhCO_2)_5(MeOH)_2](ClO_4)$	0	1.34				[16]
$[Dy_2Zn_2(L^{13})_2(OAc)_2(CO_3)_2]\cdot10CH_3OH$	0	34	2.9×10^{-6}			[17]
$[Zn(\mu\text{-}L^{14})(\mu\text{-}OAc)Dy(NO_3)_2]$	1	41 (2)	5.6×10^{-7}			[18]
$[Zn(\mu\text{-}L^{14})(\mu\text{-}OAc)Er(NO_3)_2]$	1	11.7 (3)	2.0×10^{-6}			[18]
$[Zn(\mu\text{-}L^{14})(\mu\text{-}NO_3)Er(NO_3)_2]$	1	22 (2)	5.3×10^{-8}			[18]
$[Zn(\mu\text{-}L^{14})(\mu\text{-}9\text{-}An)Dy(NO_3)_2]\cdot2CH_3CN$	1	32.1 (3)	1.9×10^{-6}			[18]
$\{(\mu_3\text{-}CO_3)_2[Zn(\mu\text{-}L^{14})Yb(H_2O)]_2\}(NO_3)_2\cdot4CH_3OH$	1	19.4 (7)	3.1×10^{-6}			[19]
$\{(\mu_3\text{-}CO_3)_2[Zn(\mu\text{-}L^{14})Yb(H_2O)]_2\}(NO_3)_2\cdot4CH_3OH$	1	27.0 (9)	8.8×10^{-7}			[19]
$[ZnDy(NO_3)_2(L^{15})_2(CH_3CO_2)]$	3.5	118.7	6.2×10^{-9}			[20]
$[ZnDy(NO_3)_2(mpko)_3(mpkoH)]$	1	33.3	2.0×10^{-7}			[21]
$[Zn_2Dy(H_3L^{16})_4]\cdot3NO_3\cdot2MeOH\cdot1.5H_2O$	1	67(3)	4.5×10^{-8}			[22]
$[La_{0.86}Tb_{0.14}(NO_3)\{Zn(L^{17})(SCN)\}_2]$	1	41.2 (4)	$7.3\ (3)\times10^{-7}$			[23]
$[La_{0.79}Dy_{0.21}(NO_3)\{Zn(L^{17})(SCN)\}_2]$	0	10 (5)	$3.14\ (10)\times10^{-8}$	0.4	3	[23]
	1	33 (4)	$1.0\ (2)\times10^{-8}$			
$[(L^{18}ZnBrDy(ovan)(NO_3)(H_2O)](H_2O)\cdot0.5(MeOH)$	0	118.5	2.8×10^{-7}			[24]

续表

$[LZnClDy(thd)_2]$	0	99.1	5.2×10^{-8}			[24]
$[(L^{19}ZnBr)_2Dy(MeOH)_2](ClO_4)$	0	63.3	2.6×10^{-7}			[24]
$[Zn(\mu\text{-}L^{20})(\mu\text{-}OAc)Nd(NO_3)_2]\cdot CH_3CN$	1	14.12	8.57×10^{-7}			[25]
$[Zn(\mu\text{-}L^{20})(\mu\text{-}OAc)Dy(NO_3)_2]\cdot CH_3CN$	1	41.55	1.79×10^{-8}			[25]
$[Zn(\mu\text{-}L^{20})(\mu\text{-}OAc)Er(NO_3)_2]\cdot CH_3CN$	1	21.0	2.28×10^{-7}			[25]
$[Zn(\mu\text{-}L^{20})(\mu\text{-}OAc)Yb(NO_3)_2]\cdot CH_3CN$	1	18.9	5.48×10^{-8}			[25]
$[ZnDy(HL^{21})(NO_3)(OAc)(CH_3OH)](NO_3)$	1	41.05	2.16×10^{-7}			[26]
$[Zn_2Dy(L^{21})(NO_3)_2(OAc)_2(H_2O)]$	1	47.69	4.60×10^{-7}			[26]
$[Zn_2Er(L^{21})(NO_3)_2(OAc)_2(H_2O)]$	1	20.81	7.48×10^{-7}			[26]
$[Zn_4Dy_2(OH)_2(L^{22})_4(OAc)_2(NO_3)_2(DMF)_3]\cdot DMF$	3	14.6	7.1×10^{-6}			[27]
$[Zn_2Dy_4(HL^{23})_4$(o-vanillin)$_2(OH)_4(CH_3OH)_2]\cdot 2NO_3\cdot 5CH_3OH$	0	56.7	4.8×10^{-7}			[28]
$[Zn_2DyL^{24}]\cdot 2ClO_4\cdot H_2O$	2	1.50	8.33×10^{-7}		2	[29]
$[Zn(\mu\text{-}L^{25})(\mu\text{-}OAc)Gd(NO_3)_2]$	1	21.6	2.92×10^{-7}			[30]
$[Zn(\mu\text{-}L^{25})(\mu\text{-}OAc)Dy(NO_3)_2]$	1	27.5	1.07×10^{-7}			[30]
$[Zn(\mu\text{-}L^{25})(\mu\text{-}OAc)Yb(NO_3)_2]$	1	13.2	5.10×10^{-7}			[30]
$[Zn_2Tb_2(L^{26})_2Cl_2(acetate)_4(MeOH)_2]$	5	26.6	3.98×10^{-7}			[31]
$[Zn_2Er_2(L^{26})L_2Cl_2(acetate)_4(MeOH)_2]\cdot 2MeOH\cdot 2H_2O$	5	17.7	6.25×10^{-7}			[31]
$[Zn_2Dy_2(L^{8})_4(CH_3COO)_2(CH_3CH_2OH)_2]\cdot 2CH_2Cl_2\cdot 0.5H_2O$	0	42.0	6.6×10^{-9}			[32]
$[Zn_2Dy_2(L^{8})_4(CH_3COO)_2(CH_3CH_2OH)_2]\cdot 4CH_2Cl_2\cdot 2CH_3OH\cdot 0.1H_2O$	0	26.0	1.26×10^{-7}			[32]
$[DyZn_2(Hhms)_2(C_6H_5COO)_4]\cdot C_6H_5COO$	0.5	12.3	1.01×10^{-6}			[33]
$\{[DyZn_2(L^{27})_2(POC)](OH)(ClO_4)\}\cdot H_2O\cdot MeOH$	0	235.3 (1)	$4.3\ (1) \times 10^{-11}$	20	3.8	[34]
	1	358.6 (7)	$3.7\ (0.3) \times 10^{-11}$			
$\{[Dy_3Zn_7(L^{28})_6(POC)_6](OH)_3(ClO_4)_2\}\cdot 9H_2O$	1	7.7 (0.2)	$1.2\ (0.1) \times 10^{-5}$			[34]
$[ZnDy(H_2L^{29})(CH_3OH)_2(NO_3)_2](NO_3)\cdot MeOH$	1	32.9	4.7×10^{-7}			[35]
$[L^{30}Zn(H_2O)Dy(acac)_2]\cdot CH_2Cl_2\cdot PF_6$	0	38.42 (5)	$1.08\ (5) \times 10^{-5}$	20	1.8	[36]
$[ZnDy(L^{31})(Pc)(ROH)]\cdot CH_3OH$	1	27.9	7.93×10^{-7}			[37]
$[ZnDy(L^{31})(Pc)(ROH)]\cdot C_2H_5OH$	1	32.5	2.74×10^{-7}			[37]
$[Zn(L^{32})_2][Dy_{10}(OH)_4(PhCOO)_{28}]$	0	15.5	4.8×10^{-6}			[38]
$[Zn_4Dy_2(L^{33})_2(L^{34})_2(N_3)_2]Cl_2\cdot 2H_2O$	1	30.66 (5)	$1.81\ (1) \times 10^{-6}$			[39]
$[Zn_4Tb_2(L^{33})_2(L^{34})_2(Cl)_2][ZnN_3Cl_3]\cdot 2H_2O$	2	8.87 (3)	2.5×10^{-4}			[39]
$[Dy_3Zn_3(Hvanox)_3(vanox)_3(NO_3)_6(H_2O)_5]\cdot 3EtOH$	2	32.34	1.24×10^{-7}			[40]
$[Er_3Zn_3(Hvanox)_3(vanox)_3(NO_3)_6(H_2O)_5]\cdot 5EtOH$	2	11.94	6.88×10^{-8}			[40]
$[Zn_2Dy_2(\mu_3\text{-}CO_3)_2(L^{35})_2(NO_3)_2(MeOH)_2]$	1.5	$U_1 = 18.8\ (0.1)\ \tau_1 = 4.4\ (0.1) \times 10^{-6}$ $U_2 = 41.0\ (1.6)\ \tau_2 = 4.3\ (0.3) \times 10^{-8}$				[41]
$[Zn_2Dy_2(\mu_3\text{-}CO_3)_2\ (L^{36})_2(NO_3)_2]\cdot 2MeOH$	1.2	$U_1 = 12.4\ (0.2)\ \tau_1 = 4.3\ (0.1) \times 10^{-6}$ $U_2 = 31.4\ (1.2)\ \tau_2 = 6.3\ (0.4) \times 10^{-9}$				[41]
$[Zn_2Tb_2(\mu_3\text{-}CO_3)_2(L^{35})_2(NO_3)_2(MeOH)_2]$	2	54.0 (1.4)	$2.8\ (0.5) \times 10^{-12}$			[41]

续表

$[Zn_2Tb_2(\mu_3\text{-}CO_3)_2(L^{36})_2(NO_3)_2]\cdot 2MeOH$	1.2	26.9 (0.7)	$2.0\ (0.3) \times 10^{-8}$	[41]
$[Zn_2Dy_2(L^{35})_2(pdm)_2(MeOH)_2](ClO_4)_2$	2	38.9 (0.7)	$6.4\ (0.1) \times 10^{-6}$	[42]
$[Zn_2Dy_2(L^{35})_2(Brpdm)_2(MeOH)_2](ClO_4)_2$	1.2	43.8 (1.4)	$4.2\ (0.2) \times 10^{-6}$	[42]
$\{Zn_2Dy_2(\mu_3\text{-}CO_3)_2(L^{37})_2(acacF_6)_2\}\cdot CH_3OH$	1.5	83.1 (1.8)	$1.2\ (0.2) \times 10^{-6}$	[43]
$[Zn_2Dy(R, R\text{-}L^{38})_2(H_2O)_4](ClO_4)_3)$	0.4	22.46	5.06×10^{-6}	[44]
$[Zn_2Tb(R, R\text{-}L^{38})_2(H_2O)_4](ClO_4)_3)$	2	38.70	1.08×10^{-7}	[44]
$[Zn_2Dy_2(R, R\text{-}L^{38})_2(CO_3)_2(NO_3)_2]\cdot 2CH_3OH$	0	19.61	2.50×10^{-7}	[44]
$[YbZn_2(SS\text{-}L^{39})_2(H_2O)_4](ClO_4)_3\cdot 5H_2O$	1	8.94	1.91×10^{-5}	[45]
$\{Zn_2Dy_2(OH)_2(L_{Schiff})_2[B(OCH_3)_4]_2Cl_2\}\cdot 2((S)\text{-binol})\cdot 2H_2O\cdot MeOH$	1.8	18.4 (3)	$1.0\ (0.1) \times 10^{-6}$	[46]
$[ZnL^{40}Dy(HO)(pyz)]_2\cdot 2CF_3O_3S\cdot 2H_2O$	0.5	84.21	3.44×10^{-7}	[47]
$[ZnL^{40}Dy(CH_3O)(aca)]_2\cdot 2CF_3O_3S\cdot 2CH_3OH$	1.1	91.79	7.54×10^{-7}	[47]
$[ZnL^{41}Dy(CH_3O)(pyz)]_2\cdot 2CF_3O_3S\cdot 2CH_3OH$	0.5	81.20	2.50×10^{-6}	[47]
$[ZnL^{41}Dy(CH_3O)(pyi)]_2\cdot 2CF_3O_3S\cdot 4CH_3OH$	1.3	91.55	4.31×10^{-8}	[47]
$[Zn_6(Dy_{0.05}Y_{0.95})_2(L^{42})_6(tea)_2(CH_3OH)_2]\cdot 6CH_3OH\cdot 8H_2O$	1	$U_1 = 52.85\ (1)$ $\tau_1 = 4.78(3) \times 10^{-12}$ $U_2 = 34.63\ (2)$ $\tau_2 = 5.82(8) \times 10^{-6}$		[48]
$[Zn_4Dy_4(L^{42})_6(pdm)_2(pdmH)_4]\cdot 10CH_3CN\cdot 5H_2O$	0	13.85 (6)	$9.58\ (3) \times 10^{-6}$	[48]
	0.6	15.00 (7)	$1.21\ (5) \times 10^{-5}$	[48]
$[Zn_4(Dy_{0.05}Y_{0.95})_4(L^{42})_6(pdm)_2(pdmH)_4]\cdot 10CH_3CN\cdot 5H_2O$	0.8	36.75 (6)	$2.68\ (8) \times 10^{-6}$	[48]
$[ZnDy(L^{43})(NO_3)_3(py)]\cdot CH_2Cl_2$	0	30.5	1.5×10^{-6}	[49]
	1	55.1	2.7×10^{-7}	[49]
$[ZnDy(L^{43})(\mu\text{-}OAc)(OAc)_2]\cdot 3H_2O$	0	59	1.1×10^{-8}	[49]
	1	107	9.7×10^{-11}	[49]
$[ZnDy(L^{43})(\mu\text{-}OAc)(OAc)(NO_3)]$	0.6	13	3.4×10^{-7}	[49]
	2	28.5	1.1×10^{-8}	[49]
$[ZnDy(L^{43})(\mu\text{-}piv)(piv)_2][ZnDy(L)(\mu\text{-}piv)(piv)(OAc)]\cdot 1.5H_2O$	0	39.3	1.8×10^{-6}	[49]
$[ZnDy(H_2L^{44})(NO_3)_3]\cdot(CH_3OH)_2$	0.6	24.49	1.44×10^{-7}	[50]
$[Zn_2Dy_2(L^{40})_4(Ac)_2(DMF)_2]\cdot 4CH_3CN$	0	18	1.40×10^{-10}	[51]
$[DyZn_2(L^{45})_2(CH_3CO_2)_4]\cdot[Zn_2Cl_4(L^{45})]\cdot H_2O$	0.5	13.53	1.78×10^{-6}	[52]
$[L^{46}Zn(CH_3COO)Dy(hfac)_2]$	1.5	45.49		[53]
$[L^{46}Zn(CH_3COO)_2Dy(dbm)]\cdot CH_2Cl_2$	0.9	69.28		[53]
$[L^{46}Zn(CH_3COO)Dy(btfa)_2]\cdot CH_2Cl_2$	1.5	101.34		[53]

H_3L^1 = 2,2’,2”-(((nitrilo-tris(ethane-2,1-diyl))tris(azanediyl))tris(methylene))tris-(4-bromo-phenol); H_2L^2 = N,N’-dimethyl-N,N’-bis(2-hydroxy-3-formyl-5-bromo-benzyl) ethylenediamine; H_2L^3 = N,N’-2,2-dimethylpropylenedi (3-methoxysalicylideneiminato); HL^4 = N,N’-bis (3-methoxysalicylidene) phenylene-1,2-diamine; HL^5 = N,N’-bis (3-methoxysalicylidene)-1,2-diaminocyclohexane; $TTTT^{Cl}$ = 2,2’,2”-(((nitrilotris(ethane-2,1-diyl)) tris (azanediyl)) tris (methylene)) tris-(4-chlorophenol); NMP = N-methyl pyrrolidone; H_2L^6 = N,N’-dimethyl-N,N’-(2-hydroxy-3-methoxy-5-methyl-benzyl) ethylenediamine; DBM^- = 1,3-diphenyl-propane-1,3-dione; H_5L^7 = a Schiff base synthesized from 2-formyl-6-hydroxymethyl-p-cresol and 1,3-diamino-2-propanol; H_2L^5 = (E)-2-ethoxy-6-(((2-hydroxyphenyl)imino)methyl)phenol; H_2L^8 = (E)-4-(*tert*-butyl)-2-((2-hydroxy-3-methoxybenzylidene)amino)phenol; H_2L^9 = N,N’-dimethyl-N,N’-bis(2-hydroxy-3,5-dimethylbenzyl) ethylenediamine; H_3L^{10} = 2-(*β*-naphthalideneamino)-2-hydroxymethyl-1-propanol; H_2L^{11} = N,N’-bis(3-methoxysalicylidene)-1,3-diaminopropane; $PyCO^{2-}$ = pyridine-2-carboxylate; m-salen = N,N’-ethylenebis (3-methoxysalicylideneamine); $(L^{Pr})^{6-}$ = hexaimine [3 + 3] macrocycle;

H_2L^{12} = 5-((E)-((2-(((E)-2-hydroxy-3-methoxybenzylidene)amino)ethyl)imino)methyl)-2-methoxyphenol; hmpH = hydroxymethylpyridine; H_2L^{13} = N,N'-bis(3-methoxysalicylidene)-1,2-cyclohexanediamine; H_2L^{14} = N,N',N"-trimethyl-N,N"-bis(2-hydroxy-3-methoxy-5-methylbenzyl)diethylenetriamine; 9-An = 9-anthracenecarboxylate anion; HL^{15} = 2-methoxy-6-[(E)-phenyliminomethyl]phenol; mpkoH = methyl 2-pyridyl ketone oxime; H_4L^{16} = [2-(2-hydroxy-3-(hydroxymethyl)-5-methylbenzylideneamino)-2-methylpropane-1,3-diol]; H_2L^{17} = a Schiff base ligand derived from o-vanillin and ethylenediamine; H_2L^{18} = N,N'-2,2-dimethylpropylenedi (3-methoxysalicylideneiminato); H_2L^{19} = 2-{(E)-[(3-{[(2E,3E)-3-(hydroxyimino)-butan-2-ylidene]amino-2,2-dimethylpropyl) imino] methyl-6-methoxyphenol; thd = 2,2,6,6-tetramethyl-3,5-heptanedionato ligand; H_2L^{20} = N,N'-dimethyl-N,N'-bis (2-hydroxy-3-formyl-5-bromo-benzyl) ethylenediamine; H_3L^{21} = 6,6'-((1E,1'E)-(((2-(5-bromo-2-hydroxy-3-methoxyphenyl)imidazolidine-1,3-diyl)bis(ethane-2,1-diyl))bis (azaneylylidene))bis(methaneylylidene))bis(4-bromo-2-methoxyphenol); H_2L^{22} = (E)-3-((2-hydroxy-3-methoxybenzylidene) amino)-naphthalen-2-ol; H_3L^{23} = 1-(2-hydroxy-4-methoxy-benzamido)-2-(2-hydroxy-3-methoxy-benzylideneamino)-ethane; H_3L^{24} = tris(((2-hydroxy-3-methoxybenzy1)amino)ethyl)amine; H_2L^{25} = N,N'-dimethyl-N,N'-bi[2-hydroxy-3-methoxy-5-methylbenzyl)-ethylenediamine; H_2L^{26} = 2-methoxy-6-[{2-(2-hydroxyethylamino)ethylimino}-methyl]phenol; H_2hms = (2-hydroxy-3-methoxybenzylidene)-semicarbazide; H_2L^{27} = N,N'-bis(3-methoxysalicylidene)-1,3-diaminopropane; POC^- = pyridin-N-oxide-4-carboxylate; H_2L^{28} = N,N'-bis(3-methoxysalicylidene)-1,2-diaminoethane; H_4L^{29} = 2,6-diacetylpyridine-bis[2-(semicarbazono) propionylhydrazone]; H_2L^{30} = N,N'-bis(2-oxy-3-methoxybenzylidene)-1,2-phenylenediamine; H_3L^{31} = 1,1,1-tris [(salicylideneamino)methyl] ethane; H_2Pc = phthalocyanine; L^{32} = 4-([2,2': 6',2"-terpyridin]-4'-yl) phenol; L^{33} and L^{34} were synthesised from N1,N3-bis(3-methoxysalicylidene)diethylenetriamine; H_2vanox = methoxysalicylaldehyde; H_2L^{35} = N,N'-bis(3-methoxysalicylidene)-1,3-diaminopropane; H_2L^{36} = N,N'-bis(3-methoxysalicylidene)-1,2-diaminoethane; H_2pdm = 2,6-pyridinedimethanol; H_2Brpdm = (4-bromopyridine-2,6-diyl)dimethanol; H_2L^{37} = N,N'-dimethyl-N,N'-(2-hydroxy-3-methoxy-5-methylbenzyl) ethylenediamine; $HacacF_6$ = hexafluoroacetylacetone; H_2L^{38} = cyclohexane-1,2-diylbis(azanediyl)bis-(methylene)bis(2-methoxyphenol); SS-H_2L^{39} = ((SS)-cyclohexane-1,2-diylbis(azanediyl))-bis(methylene))-bis(2-methoxyphenol); H_2L_{Schiff} = 2-((Z)-(3-((Z)-2-hydroxy-3-methoxybenzylideneamino) propylimino)methyl)-6-methoxyphenol; (S)-binol = (S)-1,1'-binaphthalene-2,2'-diol; L^{40} = N,N'-bis(salicylidene)ethylenediamine; L^{41} = N,N'-bis(3-methoxysalicylidene)phenylene-1,2-diamine; pyz = pyrazinehydroxamic acid; aca = acetohydroxamic acid; pyi = pyridiniumhydroxamic acid; H_2L^{42} = N-3-methoxysalicylidene-2-amino-3-hydroxypyridine; H_2L^{43} = N,N'-bis(3-methoxy-5-methylsalicylidene)-1,2-phenylenediamine; H_4L^{44} = N,N',N",N"'-tetra(2-hydroxy-3-methoxy-5-methylbenzyl)-1,4,7,10-tetraazacyclododecane; HL^{45} = (E)-2-methoxy-6-(((pyridine-2-ylmethyl)imino)methyl)phenol; H_2L^{46} = N,N'-bis(3-methoxysalicylidene)-1,2-phenylenediamine; dbm = dibenzoylmethane; btfa = benzoyltrifluoride acetone.

Zn-Ln 单分子磁体(SMMs)表现出多种拓扑结构，其中以[Zn_2Dy]配合物为主。2013 年，童明良研究团队报道了一例配合物[$Zn_2Dy(L^1)_2(MeOH)]\cdot NO_3\cdot 3MeOH\cdot H_2O$ (**1**，H_3L^1 = 2,2',2''-(((三(乙烷-2,1-二基)氮基)三亚氨基)三亚甲基)三(4-溴苯酚)) [1]。配合物 **1** 可以通过失去甲醇溶剂分子进行单晶转变，生成[$Zn_2Dy(L1)_2]NO_3\cdot H_2O$ (**2**)。同样地，**2** 可以通过浸入甲醇溶剂中转化回 **1**。在配合物 **1** 中，Dy^{III} 呈五角双锥构型(近似 D_{5h} 对称性)。当甲醇分子移除后，两个桥联的酚氧基团更接近 Dy^{III}，导致 Dy^{III} 的配位几何转变为八面体(近似 O_h 对称性)，而 Zn^{II} 则从八面体(近似 O_h 对称性)转变为扭曲的三角双锥(近似 D_{3h} 对称性) (图 1)。在零磁场下，化合物 **1** 的交流磁化率虚部(out-of-phase)信号在 30 K 以下表现出明显的温度和频率依赖性，有效能垒高达 439 K。而在化合物 **2** 中，Dy^{III} 局部对称性的显著变化导致在零磁场下虚部信号的峰值消失。然而，在施加 1.2 kOe 的外磁场时，虚部信号的峰值出现，但其 AC 峰值温度明显低于 **1**。理论计算表明，D_{5h} 构型表现出完美的轴向对称性，揭示了量子隧穿(QTM)被完全抑制，这是 **1** 中较高能垒的原因之一。相比之下，八面体几何结构则是各向同性的，导致 **2** 中弛豫速度加快。

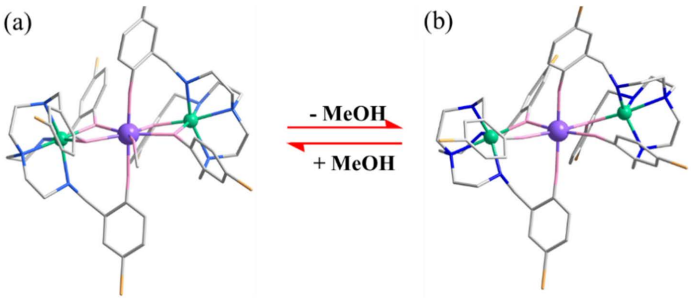

Figure 1. The molecular structure of **1** and **2**
图 1. **1** 和 **2** 的分子结构图

2014 年，Enrique Colacio 等报道了一种三核配合物[ZnCl(μ-L^2)Dy(μ-L^2)ClZn][$ZnCl_3(CH_3OH)$]·$3CH_3OH$ (**3**，H_2L^2 = N,N'-二甲基-N,N'-双(2-羟基-3-甲酰基-5-溴苄基)乙二胺) [2]。在三核阳离子单元[ZnCl(μ-L^2)Dy(μ-L^2)ClZn]$^+$中，两个[ZnCl(L^2)]$^-$单元通过配体 H_2L^2 中的酚氧基和醛氧原子与 Dy^{III} 配位，Dy^{III} 处于{O_8}四方反棱柱的配位环境中。Zn^{II} 位于由 H_2L^2 提供的{N_2O_2}配位环境中，并通过氯离子进一步连接，呈现五配位的四方锥构型(图 2(a))。配合物 **3** 的交流磁化率虚部信号在零磁场和 40 K 以下表现出频率依赖性，但在低温下出现明显的量子隧穿。通过阿伦尼乌斯定律拟合数据，确定有效能垒为 15.7 K，τ_0 为 1.4 (2) × 10^{-7} 秒。然而，所得到的能垒值低于基态与第一激发 Kramer 双重态之间的能隙，即使在施加外磁场时，QTM 也无法完全抑制，表明 QTM 过程源于分子间的磁偶极相互作用。在 1 kOe 外磁场下，配合物 **3** 的有效能垒增加到 147.3 K (图 2(b))。理论计算表明，**3** 具有稳定的强轴向 M_J = ±15/2 Kramer 双重态，且各向异性轴几乎与最短的 Dy-O 键的方向一致。这种显著的易轴各向异性解释了其在零场中较高的反转能垒。这一事实表明，QTM 过程是由分子间偶极－偶极相互作用导致的，可以合成 Dy^{III} 的同构抗磁性配合物消除分子间相互作用，从而提升单分子磁体的性能。

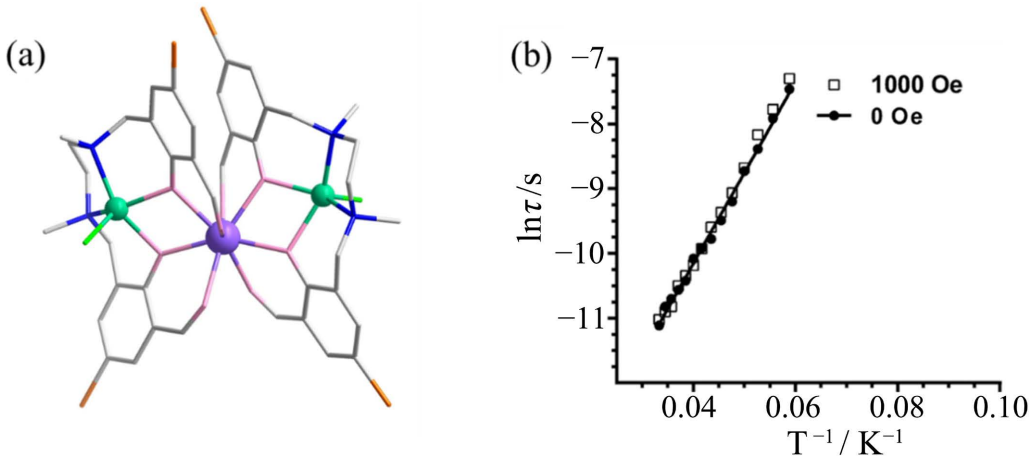

Figure 2. The molecular structure for **3** (a) and the temperature-dependence of relaxation times for **3** (b)
图 2. 3 的分子结构(a)**及其弛豫时间随温度变化的图**(b)

2015 年，Enrique Colacio 研究小组合成了三个配合物：[(L^3Zn(H_2O)$_2$Dy(H_2O)](CF_3SO_3)3 (**4**)、[(L^3ZnBr)$_2$Dy(H_2O)](ClO_4) (**5**)和[(L_3ZnCl)$_2$Dy(H_2O)](ClO_4)(MeOH) (**6**，H_2L^3 = N,N'-2,2-二甲基丙撑二(3-甲氧基水杨基亚胺基)) [3]。在配合物 **4** 中，[(L^3Zn(H_2O))$_2$Dy(H2O)]$^+$单元由两个[ZnL^3]片段组成，每个片段通过两个酚氧基氧原子和两个甲氧基连接到中央 Dy^{III} 离子。此外，Dy^{III} 的配位环境中还包含一个水分子。去质子化的配体(L^3)$^{2-}$为 Zn^{II} 提供了 N_2O_2 配位环境，并由一个水分子占据轴向位置。与 **4** 不同的是，配合物 **5** 和 **6** 中，Zn^{II} 轴向配位的水分子分别被 Br^-和 Cl^-取代。三种配合物在零磁场交流磁化率测量中均表现出单分子磁体行为，且有效能垒分别为 96.9 (6) K、146.8 (5) K、146.1 (10) K。施加 1 kOe 外磁场后，QTM 部分或完全被抑制，使 **4**、**5** 和 **6** 的有效能垒分别增加到 128.6 (5) K，214.7 K，202.4 K，**5** 的有效能垒最大，并且 **5**，**6** 都远高于 **3**。理论计算表明，这三种配合物中能垒增强的原因是 Zn^{II} 的存在，它在酚氧基氧原子上诱导了显著的电荷极化，产生了强烈的晶场，稳定了轴向 Kramers 双重态。同时，Zn^{II} 减弱了分子间相互作用并抑制了 QTM。

2016 年，高松研究团队报道了一系列 Zn-Dy-Zn 单分子磁体，即[$Zn_2(L^4)_2DyCl_3$]·$2H_2O$ (**7**，HL^4 = N,N'-双(3-甲氧基水杨醛基)苯-1,2-二胺)，[$Zn_2(L^4)$2Dy(MeOH)Br_3]·$3H_2O$ (**8**)，[$Zn_2(L^4)_2$Dy(H_2O)Br_2]·[$ZnBr_4$]$_{0.5}$ (**9**)，和[$Zn_2(L^5)_2DyCl_3$]·$2H_2O$ (**10**, HL^5 = N,N'-双(3-甲氧基水杨醛基)-1,2-二氨基环己烷) [4]。在较高温度范围内，

7~10 的交流磁化率的实部和虚部信号表现出明显的频率依赖性。然而，在较低温度下出现了显著的量子隧穿。当施加 1 kOe 的外磁场时，QTM 得到显著抑制。在 0 或 1 kOe 的磁场下，**7** 分别展现了 430 K 和 481 K 的有效能垒。**10** 表现出与 **7** 类似的弛豫行为，在零直流场下其有效能垒为 398 K。然而，**8** 和 **9** 在 ln(*τ*)对 1/T 曲线上表现出明显的非线性关系。因此，仅对高温区进行了阿伦尼乌斯定律拟合，得出了 **8** 和 **9** 的 U_{eff}/k_B 值分别为 233 K 和 121 K。此外，对 **7~10** 的磁滞回线显示在低于 8 K、6 K、4 K 和 8 K 的温度下存在磁滞现象。理论计算进一步揭示了 **7~10** 中存在一个由四个甲氧基和一个取代基组成的五元环。这个五元环几乎垂直于易轴，并且随着五元环上的电荷密度减小，轴向配体场变得更强，从而导致更显著的慢磁弛豫。含稀土元素的配合物通常具有高配位数和灵活的配位几何结构，磁性数据分析和理论计算表明，Dy (III)离子周围的电荷分布对称性是决定这些分子慢磁弛豫的关键因素，这为设计新的稀土单分子磁体提供了一个实用的思路。

2020 年，童明良研究团队报道了五个配合物，分子式为$[Zn_2Dy(TTTTCl)_2L]\cdot Anion\cdot Solv$ ($TTTT^{Cl}$ = 2,2’,2’’-(((三乙二胺)三甲基)三(4-氯苯酚))，图 3) [5]。在这五个配合物中，金属离子的非对称单元和配位环境表现出显著的相似性。每个 Zn^{II} 都呈现出扭曲的八面体构型，$TTTT^{Cl}$ 配体提供四个氮原子和两个氧原子。Dy^{III} 则仅与氧原子配位，形成压缩的五角双锥配位构型(图 4(a))。所有五个配合物都表现出典型的单分子磁体行为，其计算的有效能垒分别为 507 K、525 K、632 K、535 K 和 558 K。此外，在磁滞回线的测量中，配合物 **11~15** 显示出 12 K 至 24 K 范围内的矫顽温度(图 4(b))。值得注意的是，由于量子隧穿的存在，**11** 和 **12** 配合物的矫顽场相对较小。相比之下，配合物 **13~15** 不仅在较高温度下显示出磁滞回线，而且在扫描速率为 200 Oe/s 时展现出显著的矫顽场。从 TG-MS 分析中可以发现，配合物 **11** 和 **13** 即使失去配位的丙酮也能保持稳定，而配合物 **14** 和 **15** 一旦失去 DMF 或 NMP 端配体就会发生热分解。不同的化学稳定性可归因于分子大小的多样性、Dy(III)与配位溶剂的亲和力以及配位溶剂的沸点。因此，从这系列配合物的研究中可以推断，轴向配体场、键长和键角的调节在调控 SMM 性能方面起着重要作用[54]。

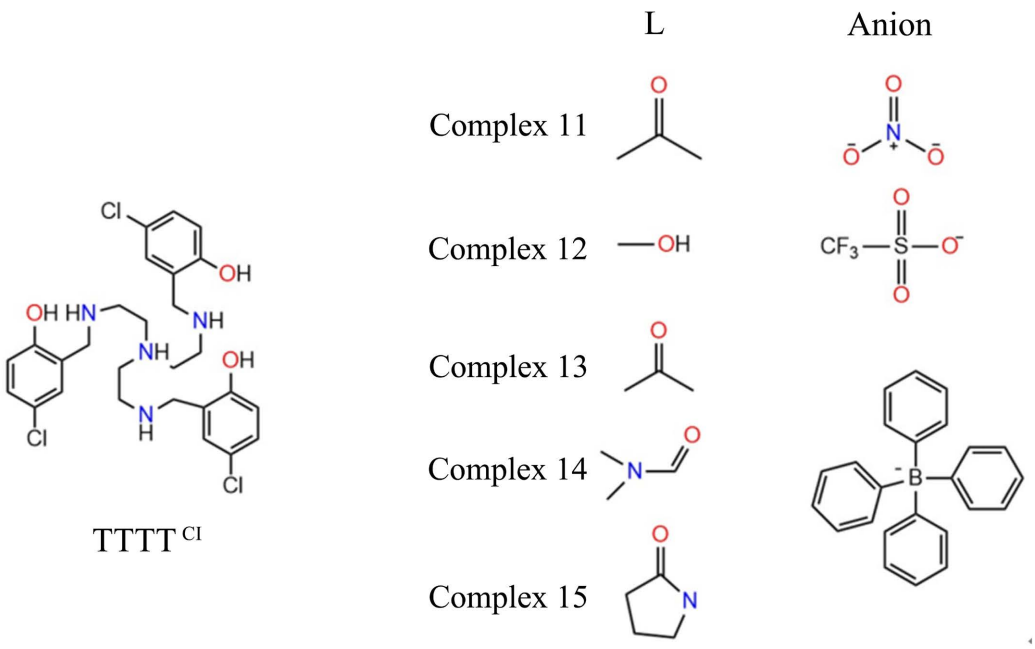

Figure 3. The ligands used in complexes **11~15**
图 3. 配合物 **11~15** 中使用的配体

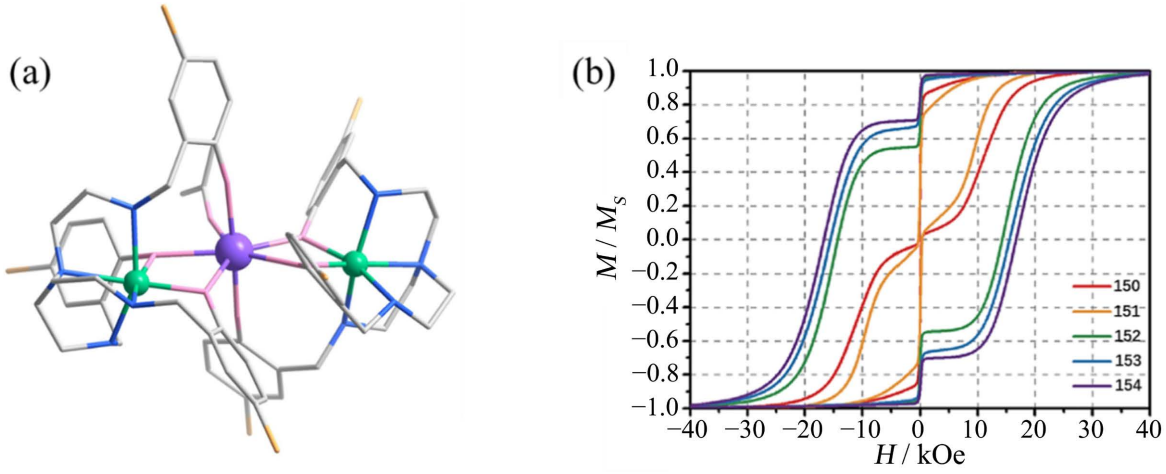

Figure 4. The molecular structure (a) and hysteresis loops (b) for complex **11**
图 4. 配合物 **11** 的分子结构图(a)和磁滞回线图(b)

2014 年，寇会忠研究团队报道了一例双核 3d-4f 单分子磁体，即[ZnDy(L^6)(DBM)$_3$] (**16**，H_2L^6 = N,N'-二甲基-N,N'-(2-羟基-3-甲氧基-5-甲基苄基)乙二胺，DBM^- = 1,3-二苯基丙烷-1,3-二酮) [6]。在该配合物中，去质子化的配体$(L^6)^{2-}$包裹 Zn^{II}，占据内部 N_2O_2 配位位点，而 Dy^{III} 则位于外部 O4 配位位点。Dy^{III} 与 Zn^{II} 之间的连接由配体$(L^6)^{2-}$中的两个酚氧基团实现(图 5(a))。此外，三个 DBM^-阴离子占据了 Zn^{II} 和 Dy^{III} 的剩余配位位点，导致 Zn^{II} 和 Dy^{III} 分别呈现近似六配位的扭曲八面体构型和八配位的三角十二面体构型。这一结果表明分子内磁交换在单分子磁体中是重要的。动态磁化率测量显示 **16** 在零场下有频率依赖的虚部信号，但是未观察到峰值。施加 2 kOe 的外磁场后，**16** 在 8 K 以下表现出 SMM 行为，按照 Arrhenius 定律拟合的有效能垒为 36.5 K，前指数因子 $\tau_0 = 1.56 \times 10^{-6}$ s (图 5(b))。单核 Dy^{III} 配合物的 $\chi_M T$ 值随温度降低而增加的情况并不常见。直流磁化率测试证实了 Dy^{III} 的磁各向异性和配体场效应。尽管 Dy^{III} 的配位环境对称性较低(D_{2d})，Dy-O 键长介于 2.276 (2)~2.345 (2) Å 之间，产生了适当的轴向配体场作用于 Dy^{III}。

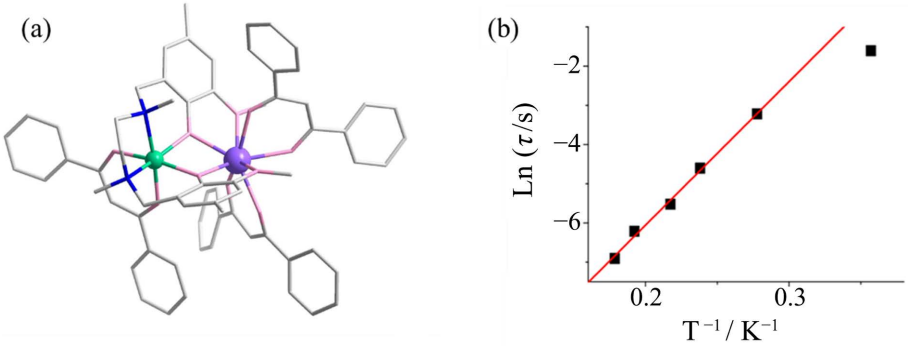

Figure 5. The molecular structure (a) and ln(τ) *vs* T^{-1} plot (b) of **16**
图 5. **16** 的分子结构图(a)和 ln(τ) *vs* T^{-1} 图(b)

2016 年，Lorenzo Sorace 报道了一例双核配合物[ZnDy(H_4L^7)$_2$](NO_3)$_3$·6H_2O (**17**，H_5L_7 为由 2-甲醛-6-羟甲基-p-甲酚和 1,3-二氨基-2-丙醇合成的 Schiff 碱) [7]。在配合物 **17** 中，Dy^{III} 和 Zn^{II} 由两个来自两个 H_5L^7 配体的酚氧基氧原子桥联。此外，H_5L^7 提供了与 Dy^{III} 配位的酚氧基和苄氧基，使 Dy^{III} 的配位构型接近四方反棱柱。Zn^{II} 呈现扭曲的八面体配位构型，其配位的氮和氧原子均来源于 H5L^7 配体(图 6(a))。在零场和施加外场的情况下，配合物 **17** 均表现出显著的单分子磁体行为。在 Arrhenius 图中，**17** 的弛豫

时间在高温区表现出线性依赖性，表明 Orbach 过程占主导，有效能垒为 270.3 K 和前指数因子 τ_0 = 2.67 × 10^{-10} s (图 6(b))。施加直流场预计会抑制磁化的量子隧穿，使热激活机制占主导。与这种解释一致，在热激活区域施加场时没有观察到明显变化。还可以进一步注意到，即使在施加场的情况下，在中间温度区域也存在明显偏离线性行为的情况，这表明不同的热激活过程同时起作用。此外，当引入 Y^{III} 进行稀释后，尽管 Dy^{III} 在体系中被稀释至仅 1%，晶格中短的 Dy^{III}-Dy^{III} 距离仍然使得偶极相互作用无法完全忽略。此外，**17** 中顺磁性 Zn^{II} 的存在显著诱导了氧原子的电荷极化，加上 Dy^{III} 的晶体 C_2 对称轴的存在，使配合物展现出 SMM 的行为。

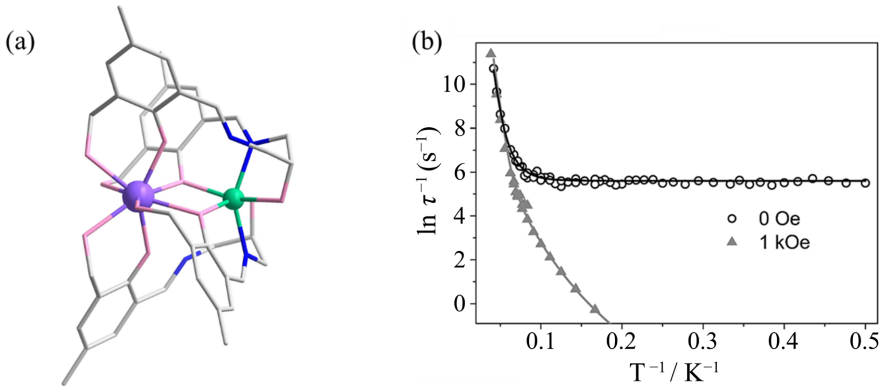

Figure 6. The molecular structure (a) and ln(τ) *vs* T^{-1} plot (b) of **17**
图 6. **17** 的分子结构图(a)和 ln(τ) *vs* T^{-1} 图(b)

2017 年，宋友研究团队合成了配合物[$Dy_2Zn_2(L^5)_4(NO_3)_2(CH_3OH)_2$] (**18**)，其配体 H_2L^5 与配合物 **10** 中使用的相同[8]。在结构上，配合物 **18** 的 Dy^{III} 在其赤道平面上呈现出扭曲的五元环结构，两个硝酸根 O 一个酚羟基 O 轴向配位，形成八配位的呼啦圈构型，但与 **24** 中 Zn^{II} 配位 DMF 不同，**18** 中 Zn^{II} 配位的是甲醇(MeOH) (图 7(a))。在配合物 **18** 中，两个 Dy^{III} 之间通过两个顺磁性的 Zn^{II} 发生铁磁偶极相互作用。在交流磁化率测试中，实部和虚部信号均表现出显著的频率依赖性。在 17~22 K 的温度范围内按 Arrhenius 定律拟合得到有效能垒为 78 K，τ_0 = 4.59 × 10^{-6} s。值得注意的是，配合物 **18** 在低温下表现出明显的量子隧穿效应。施加 1 kOe 的外磁场有效抑制了 QTM，使热激发弛豫过程的能垒上升至 96 K。此外，在 4 K 以下，**18** 表现出蝴蝶形的磁滞回线(图 7(b))。理论计算表明，**18** 的能垒与 Dy^{III} 离子激发态 Kramers 双重态的弛豫过程有关，Dy^{III}-Dy^{III} 各向异性偶极相互作用改变了基态的隧穿分裂，从而部分抑制了 QTM。

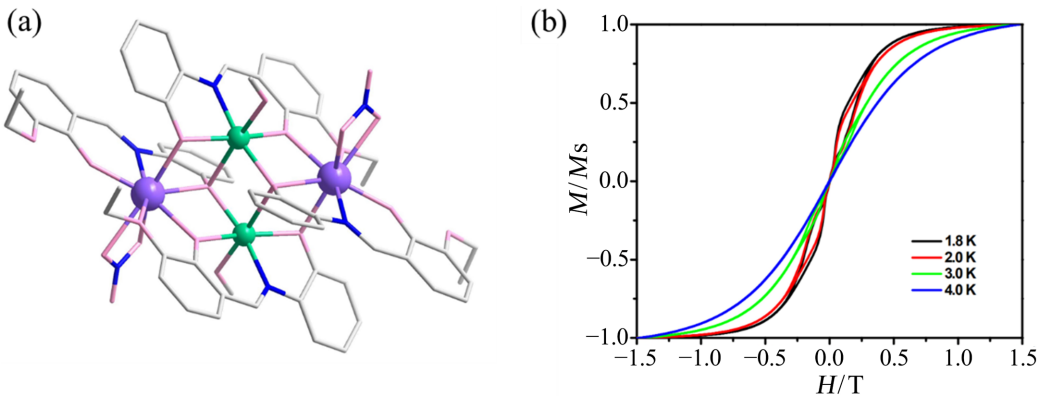

Figure 7. The molecular structure (a) and hysteresis loops (b) for complex **18**
图 7. 配合物 **18** 的分子结构图(a)和磁滞回线图(b)

2019 年，两个四核配合物[$Zn_2Dy_2(L^8)_4(NO_3)_2(CH_3OH)_2$]·2$CH_3COCH_3$(**19**，$H_2L^8$ = (E)-4-(tert-butyl)-2-((2-hydroxy-3-methoxybenzylidene)amino)phenol)和[$Zn_2Dy_2(L^8)_4(CH_3COO)_2(CH_3CH_2OH)_2$]·4$CH_3COCH_3$ (**20**) [9]。这两种配合物在金属核心排列上具有显著相似性，[Zn_2DyO_4]单元通过两个双桥接的酚氧原子和两个三桥接的酚氧原子相互连接，同时两个具有缺陷的立方体共享一个共同的{Zn_2O_2}平面。在 **19** 和 **20** 中，每个 Zn^{II} 离子都是八面体配位构型。在 **19** 中，Dy^{III} 通过三种去质子化配体和一个以二齿螯合方式配位的硝酸根离子配体进行配位。在 **20** 中，类似的二齿螯合方式的乙酸根离子配体替代了 **19** 中的硝酸根离子配体。因此，两个配合物中 Dy^{III} 的配位几何形状接近于双帽三棱柱。**19** 中观察到两个 Dy^{III} 之间存在弱铁磁相互作用，而 **19** 可能存在分子间反铁磁交换相互作用。此外，这两个配合物均表现出显著的磁各向异性和/或低的激发态，表现出单分子磁性行为。在较高温度下，有效能垒分别为 31.4 K 和 57.2 K。然而，在较低温度下，这两种配合物表现出不同的弛豫行为。理论计算表明，**19** 和 **20** 中不同的弛豫行为源于与 Dy^{III} 配位的阴离子的变化。此外，与 **20** 中的乙酸根离子配体的键长相比，**19** 中硝酸根离子配体的螯合键长较短，从而使得 **19** 的能垒显著高于 **20**。

2014 年，Muktimoy Chaudhury 等报道了一种四核配合物[$Zn_2(L^9)_2(PhCOO)_2Dy_2(hfac)_4$] (**21**，$H_2L^9$ = N,N'-二甲基-N,N'-双(2-羟基-3,5-二甲基苄基)乙烯二胺) [10]。在该配合物中，四个金属离子以交替方式排列在菱形核心的四个角落。来自苯甲酸盐配体的两个羧酸氧原子以 μ_4-η^2:η^2 模式配位，连接中心的四个金属离子(图 8(a))。此外，在配合物 **21** 中，Dy^{III} 离子之间存在反铁磁耦合。通过交流磁化率测量确认其慢磁弛豫行为，与配合物 **7**~**10** 类似，得到 U_{eff}/k_B = 47.9 K 和 $\tau_0 = 2.75 \times 10^{-7}$ s (图 8(b))，可以归因于 Dy^{III} 的强各向异性。

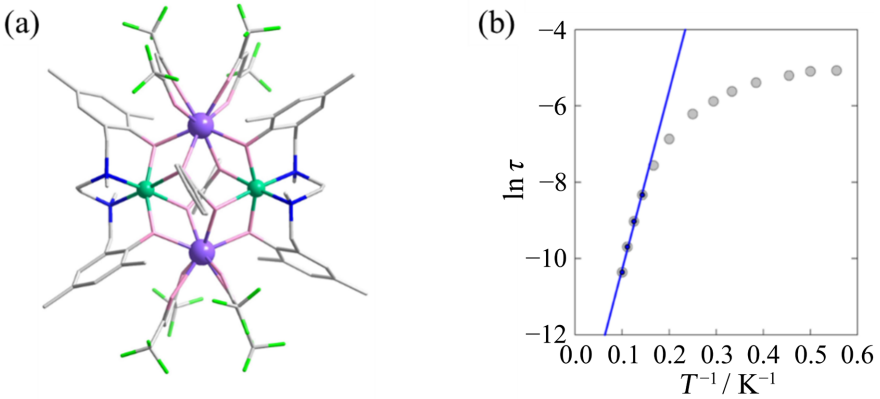

Figure 8. The molecular structure (a) and ln(τ) *vs* T^{-1} plot (b) of **21**
图 8. **21** 的分子结构图(a)和 ln(τ) *vs* T^{-1} 图(b)

2019 年，Constantinos J. M.等报道了一种新型十核配合物，分子式为[$Dy_6Zn_4O_2(L^{10})_2(HL_{10})_2(OAc)_8(CH_3O)_4(H_2O)_2$]·4MeOH(**22**，$H_3L^{10}$ = 2-(β-萘醛胺)-2-羟甲基-1-丙醇) [11]。该配合物中，Dy^{III} 离子构成了畸变的八面体金属骨架，外围是四个抗磁的 Zn^{II} 离子。对 **22** 的磁化率测量表明，配合物中存在弱的反铁磁相互作用，在零磁场下，**22** 显示出单分子磁体的行为，有效能垒为 U_{eff} = 43 K，$\tau_0 = 1 \times 10^{-5}$ s。

2020 年，一个手性配合物[$Zn_3Dy_3(O_2)(L^{11})_3(PyCO_2)_3$](OH)$_2$($ClO_4$)$_2$·8$H_2O$ (**23**, H_2L^{11} = N,N'-双(3-甲氧基水杨醛亚胺)-1,3-二氨丙烷，$PyCO_2^-$ = 吡啶-2-羧酸根) [12]。该配合物包含两个镜像对称性的对映异构单晶，其中 1-R 的晶体结构与 1-S 相同。在 1-S 对映异构体中，[ZnL^{11}]单元通过两个酚氧原子和两个甲氧基氧原子连接 Dy^{3+}离子，而 $PyCO_2^-$配体以 μ_3-η^1:η^2:η^1 模式连接两个 Dy^{3+}离子和一个 Zn^{2+}离子。此外，过氧阴离子以 μ_3-η^3:η^3 方式配位，形成[Dy_3]等边三角形的顶部和底部帽状结构。值得注意的是，这些配体本

身并不具备手性，但由于存在高氯酸根阴离子，使配合物具有手性。通过阴离子和阳离子的协同取向可以为离子配合物获得手性，这是从非手性配体组装新型手性配合物的一种可行方法。在 **23** 中，Dy^{3+}离子之间存在铁磁相互作用，并且在 1 kOe 磁场下表现出单分子磁体行为，其有效能垒约为 100.4 (3.9) K，τ_0 = 1.2 (0.4) × 10^{-8} s。

3. 结论

Zn-Ln 单分子磁体作为一类具有独特磁学性质的材料，吸引了研究者们广泛的研究兴趣[55]-[58]。目前已报道的 Zn-Ln 单分子磁体还相对较少并且因为锌作为一种过渡金属其本身不具备磁性，研究主要集中在理解磁体的磁学行为和性质，并改进合成和制备技术。虽然已取得了一些重要的进展，但仍面临着合成方法不成熟、磁性行为理解不够全面等问题。

综合以上研究进展，本文综述了不同结构类型且单分子磁体性能优异的 Zn-Ln 单分子磁体随着科学技术的不断进步，可以将 Zn-Ln 单分子磁体纳入纳米技术中，实现更高级别的磁性控制，并用于纳米电子学和纳米磁性器件，为稀土－过渡异金属单分子磁体的应用和发展做出了重要贡献。

基金项目

江苏省研究生科研与实践创新计划项目(KYCX24_3546、SJCX24_1995、SJCX24_1992)资助，南通大学大学生创新创业训练计划项目(2024116)，南通大学大型仪器开放基金资助(KFJN2471、KFJN2437)，感谢南通大学分析测试中心。

参考文献

[1] Liu, J., Chen, Y., Zheng, Y., Lin, W., Ungur, L., Wernsdorfer, W., *et al*. (2013) Switching the Anisotropy Barrier of a Single-Ion Magnet by Symmetry Change from Quasi-D_{5h} to Quasi-O_h. *Chemical Science*, **4**, 3310-3316. https://doi.org/10.1039/c3sc50843a

[2] Oyarzabal, I., Ruiz, J., Seco, J.M., Evangelisti, M., Camón, A., Ruiz, E., *et al*. (2014) Rational Electrostatic Design of Easy-Axis Magnetic Anisotropy in a Zn^{II}-Dy^{III}-Zn^{II} Single-Molecule Magnet with a High Energy Barrier. *Chemistry—A European Journal*, **20**, 14262-14269. https://doi.org/10.1002/chem.201403670

[3] Costes, J.P., Titos-Padilla, S., Oyarzabal, I., Gupta, T., Duhayon, C., Rajaraman, G., *et a*l. (2015) Analysis of the Role of Peripheral Ligands Coordinated to Zn^{II} in Enhancing the Energy Barrier in Luminescent Linear Trinuclear Zn-Dy-Zn Single-Molecule Magnets. *Chemistry—A European Journal*, **21**, 15785-15796. https://doi.org/10.1002/chem.201501500

[4] Sun, W., Yan, P., Jiang, S., Wang, B., Zhang, Y., Li, H., *et al*. (2016) High Symmetry or Low Symmetry, That Is the Question—High Performance Dy(III) Single-Ion Magnets by Electrostatic Potential Design. *Chemical Science*, **7**, 684-691. https://doi.org/10.1039/c5sc02986d

[5] Huang, G., Ruan, Z., Zheng, J., Chen, Y., Wu, S., Liu, J., *et al*. (2020) Seeking Magneto-Structural Correlations in Easily Tailored Pentagonal Bipyramid Dy(III) Single-Ion Magnets. *Science China Chemistry*, **63**, 1066-1074. https://doi.org/10.1007/s11426-020-9746-x

[6] Xie, Q., Wu, S., Shi, W., Liu, C., Cui, A. and Kou, H. (2014) Heterodinuclear M^{II}-Ln^{III} Single Molecule Magnets Constructed from Exchange-Coupled Single Ion Magnets. *Dalton Transactions*, **43**, Article 11309. https://doi.org/10.1039/c4dt00740a

[7] Amjad, A., Madalan, A.M., Andruh, M., Caneschi, A. and Sorace, L. (2016) Slow Relaxation of Magnetization in an Isostructural Series of Zinc-Lanthanide Complexes: An Integrated EPR and AC Susceptibility Study. *Chemistry—A European Journal*, **22**, 12849-12858. https://doi.org/10.1002/chem.201601996

[8] Li, J., Wei, R., Pu, T., Cao, F., Yang, L., Han, Y., *et al*. (2017) Tuning Quantum Tunnelling of Magnetization through 3d-4f Magnetic Interactions: An Alternative Approach for Manipulating Single-Molecule Magnetism. *Inorganic Chemistry Frontiers*, **4**, 114-122. https://doi.org/10.1039/c6qi00407e

[9] Ke, H., Wei, W., Yang, Y., Zhang, J., Zhang, Y., Xie, G., *et al*. (2019) Effect of Coordination Anion Substitutions on Relaxation Dynamics of Defect Dicubane Zn_2Dy_2 Tetranuclear Clusters. *Dalton Transactions*, **48**, 7844-7852. https://doi.org/10.1039/c9dt01074b

[10] Abtab, S.M.T., Majee, M.C., Maity, M., Titiš, J., Boča, R. and Chaudhury, M. (2014) Tetranuclear Hetero-Metal [$Co^{II}_2Ln^{III}_2$] (Ln=Gd, Tb, Dy, Ho, La) Complexes Involving Carboxylato Bridges in a Rare M_4-η^2:η^2 Mode: Synthesis, Crystal Structures, and Magnetic Properties. *Inorganic Chemistry*, **53**, 1295-1306. https://doi.org/10.1021/ic401484d

[11] Stavgianoudaki, N., Siczek, M., Lis, T., Lorusso, G., Evangelisti, M. and Milios, C.J. (2019) A Decanuclear [$Dy^{III}_6Zn^{II}_4$] Cluster: A {Zn^{II}_4} Rectangle Surrounding an Octahedral {Dy^{III}_6} Single Molecule Magnet. *Dalton Transactions*, **48**, 3566-3570. https://doi.org/10.1039/c9dt00440h

[12] Liu, C., Zhang, D., Hao, X. and Zhu, D. (2020) Assembly of Chiral 3d-4f Wheel-Like Cluster Complexes with Achiral Ligands: Single-Molecule Magnetic Behavior and Magnetocaloric Effect. *Inorganic Chemistry Frontiers*, **7**, 3340-3351. https://doi.org/10.1039/d0qi00632g

[13] Burrow, C.E., Burchell, T.J., Lin, P., Habib, F., Wernsdorfer, W., Clérac, R., *et al*. (2009) Salen-Based [Zn_2Ln_3] Complexes with Fluorescence and Single-Molecule-Magnet Properties. *Inorganic Chemistry*, **48**, 8051-8053. https://doi.org/10.1021/ic9007944

[14] Feltham, H.L.C., Lan, Y., Klöwer, F., Ungur, L., Chibotaru, L.F., Powell, A.K., *et al*. (2011) A Non-Sandwiched Macrocyclic Monolanthanide Single-Molecule Magnet: The Key Role of Axiality. *Chemistry—A European Journal*, **17**, 4362-4365. https://doi.org/10.1002/chem.201100438

[15] Maeda, M., Hino, S., Yamashita, K., Kataoka, Y., Nakano, M., Yamamura, T., *et al*. (2012) Correlation between Slow Magnetic Relaxation and the Coordination Structures of a Family of Linear Trinuclear Zn(II)-Ln(III)-Zn(II) Complexes (Ln=Tb, Dy, Ho, Er, Tm and Yb). *Dalton Transactions*, **41**, Article 13640. https://doi.org/10.1039/c2dt31399e

[16] Yu, W., Lee, G. and Yang, E. (2013) Systematic Studies of the Structures and Magnetic Properties for a Family of Cubane Complexes with the Formula: [M_2Ln_2] (Ln=Dy, Gd; M=Ni, Zn) and [Ni_2Y_2]. *Dalton Transactions*, **42**, Article 3941. https://doi.org/10.1039/c2dt32688d

[17] Zhang, P., Zhang, L., Lin, S. and Tang, J. (2013) Tetranuclear [MDy]$_2$ Compounds and Their Dinuclear [MDy] (M=Zn/Cu) Building Units: Their Assembly, Structures, and Magnetic Properties. *Inorganic Chemistry*, **52**, 6595-6602. https://doi.org/10.1021/ic400620j

[18] Palacios, M.A., Titos-Padilla, S., Ruiz, J., Herrera, J.M., Pope, S.J.A., Brechin, E.K., *et al*. (2013) Bifunctional $Zn^{II}Ln^{III}$ Dinuclear Complexes Combining Field Induced SMM Behavior and Luminescence: Enhanced NIR Lanthanide Emission by 9-Anthracene Carboxylate Bridging Ligands. *Inorganic Chemistry*, **53**, 1465-1474. https://doi.org/10.1021/ic402597s

[19] Ruiz, J., Lorusso, G., Evangelisti, M., Brechin, E.K., Pope, S.J.A. and Colacio, E. (2014) Closely-Related $Zn^{II}_2Ln^{III}_2$ Complexes (Ln^{III}=Gd, Yb) with Either Magnetic Refrigerant or Luminescent Single-Molecule Magnet Properties. *Inorganic Chemistry*, **53**, 3586-3594. https://doi.org/10.1021/ic403097s

[20] Upadhyay, A., Singh, S.K., Das, C., Mondol, R., Langley, S.K., Murray, K.S., *et al*. (2014) Enhancing the Effective Energy Barrier of a Dy(III) SMM Using a Bridged Diamagnetic Zn(II) Ion. *Chemical Communications*, **50**, 8838-8841. https://doi.org/10.1039/c4cc02094d

[21] Anastasiadis, N.C., Polyzou, C.D., Kostakis, G.E., Bekiari, V., Lan, Y., Perlepes, S.P., *et al*. (2015) Dinuclear Lanthanide(III)/Zinc(II) Complexes with Methyl 2-Pyridyl Ketone Oxime. *Dalton Transactions*, **44**, 19791-19795. https://doi.org/10.1039/c5dt03663a

[22] Das, S., Bejoymohandas, K.S., Dey, A., Biswas, S., Reddy, M.L.P., Morales, R., *et al*. (2015) Amending the Anisotropy Barrier and Luminescence Behavior of Heterometallic Trinuclear Linear [M^{II}-Ln^{III}-M^{II}] (Ln^{III}=Gd, Tb, Dy; M^{II}=Mg/Zn) Complexes by Change from Divalent Paramagnetic to Diamagnetic Metal Ions. *Chemistry—A European Journal*, **21**, 6449-6464. https://doi.org/10.1002/chem.201406666

[23] Then, P.L., Takehara, C., Kataoka, Y., Nakano, M., Yamamura, T. and Kajiwara, T. (2015) Structural Switching from Paramagnetic to Single-Molecule Magnet Behaviour of Lnzn2 Trinuclear Complexes. *Dalton Transactions*, **44**, 18038-18048. https://doi.org/10.1039/c5dt02965a

[24] Costes, J.P., Titos-Padilla, S., Oyarzabal, I., Gupta, T., Duhayon, C., Rajaraman, G., *et al*. (2016) Effect of Ligand Substitution around the Dyiii on the SMM Properties of Dual-Luminescent Zn-Dy and Zn-Dy-Zn Complexes with Large Anisotropy Energy Barriers: A Combined Theoretical and Experimental Magnetostructural Study. *Inorganic Chemistry*, **55**, 4428-4440. https://doi.org/10.1021/acs.inorgchem.6b00228

[25] Oyarzabal, I., Artetxe, B., Rodríguez-Diéguez, A., García, J.Á., Seco, J.M. and Colacio, E. (2016) A Family of Acetato-Diphenoxo Triply Bridged Dimetallic Zniilniiicomplexes: SMM Behavior and Luminescent Properties. *Dalton Transactions*, **45**, 9712-9726. https://doi.org/10.1039/c6dt01327a

[26] Fondo, M., Corredoira-Vázquez, J., García-Deibe, A.M., Sanmartín-Matalobos, J., Herrera, J.M. and Colacio, E. (2017) Designing Ligands to Isolate Znln and Zn2ln Complexes: Field-Induced Single-Ion Magnet Behavior of the Zndy, Zn_2Dy, and Zn_2Er Analogues. *Inorganic Chemistry*, **56**, 5646-5656. https://doi.org/10.1021/acs.inorgchem.7b00165

[27] Griffiths, K., Mayans, J., Shipman, M.A., Tizzard, G.J., Coles, S.J., Blight, B.A., *et al*. (2017) Four New Families of

Polynuclear Zn-Ln Coordination Clusters. Synthetic, Topological, Magnetic, and Luminescent Aspects. *Crystal Growth & Design*, **17**, 1524-1538. https://doi.org/10.1021/acs.cgd.6b01401

[28] Song, X., Liu, P., Wang, C., Liu, Y., Liu, W. and Zhang, M. (2017) Three Sandwich-Type Zinc(II)-Lanthanide(III) Clusters: Structures, Luminescence and Magnetic Properties. *RSC Advances*, **7**, 22692-22698. https://doi.org/10.1039/c7ra01469d

[29] Wen, H.R., Dong, P.P., Liu, S.J., *et al*. (2017) 3d-4f Heterometallic Trinuclear Complexes Derived from Amine-Phenol Tripodal Ligands Exhibiting Magnetic and Luminescent Properties. *Dalton Transactions*, **46**, 1153-1162. https://doi.org/10.1039/C6DT04027F

[30] Zabala-Lekuona, A., Cepeda, J., Oyarzabal, I., Rodríguez-Diéguez, A., García, J.A., Seco, J.M., *et al*. (2017) Rational Design of Triple-Bridged Dinuclear $Zn^{II}Ln^{III}$-Based Complexes: A Structural, Magnetic and Luminescence Study. *CrystEngComm*, **19**, 256-264. https://doi.org/10.1039/c6ce02240e

[31] Ghosh, S., Hari, N., Pinkowicz, D., Fitta, M. and Mohanta, S. (2018) Syntheses, Crystal Structures and Magnetic Properties of a Series of $Zn^{II}_2Ln^{III}_2$ Compounds (Ln = Gd, Tb, Dy, Ho and Er): Contrasting Structural and Magnetic Features. *New Journal of Chemistry*, **42**, 15917-15929. https://doi.org/10.1039/c8nj02532k

[32] Ke, H., Wei, W., Zhang, Y.Q., *et al*. ((2018) Influence of Alcoholic Solvent and Acetate Anion Coordination Mode Variations on Structures and Magnetic Properties of Heterometallic Zn_2Dy_2 Tetranuclear Clusters. *Dalton Transactions*, **47**, 16616-16626. https://doi.org/10.1039/C8DT03983F

[33] Li, M., Wu, H., Wei, Q., Ke, H., Yin, B., Zhang, S., *et al*. (2018) Two $\{Zn^{II}_2Dy^{III}\}$ Complexes Supported by Monophenoxido/Dicarboxylate Bridges with Multiple Relaxation Processes: Carboxylato Ancillary Ligand-Controlled Magnetic Anisotropy in Square Antiprismatic Dy^{III} Species. *Dalton Transactions*, **47**, 9482-9491. https://doi.org/10.1039/c8dt01842a

[34] Liu, C., Zhang, D., Su, J., Zhang, Y. and Zhu, D. (2018) Single-Molecule Magnet Behavior of 1D Coordination Polymers Based on $DyZn_2(Salen)_2$ Units and Pyridin-n-Oxide-4-Carboxylate: Structural Divergence and Magnetic Regulation. *Inorganic Chemistry*, **57**, 11077-11086. https://doi.org/10.1021/acs.inorgchem.8b01653

[35] Shen, F., Li, H., Miao, H., Shao, D., Wei, X., Shi, L., *et al*. (2018) Heterometallic $M^{II}Ln^{III}$ (M=Co/Zn; Ln=Dy/y) Complexes with Pentagonal Bipyramidal 3d Centers: Syntheses, Structures, and Magnetic Properties. *Inorganic Chemistry*, **57**, 15526-15536. https://doi.org/10.1021/acs.inorgchem.8b02875

[36] Yang, J., Tian, Y., Tao, J., Chen, P., Li, H., Zhang, Y., *et al*. (2018) Modulation of the Coordination Environment around the Magnetic Easy Axis Leads to Significant Magnetic Relaxations in a Series of 3d-4f Schiff Complexes. *Inorganic Chemistry*, **57**, 8065-8077. https://doi.org/10.1021/acs.inorgchem.8b00056

[37] Ge, J., Chen, Z., Qiu, Y., Huo, D., Zhang, Y., Wang, P., *et al*. (2019) Modulating Magnetic Property of Phthalocyanine Supported M^{II}-Dy^{III} (M=Ni, Zn) Heterodinuclear Complexes. *Inorganic Chemistry*, **58**, 9387-9396. https://doi.org/10.1021/acs.inorgchem.9b01179

[38] Xie, X., Yang, L. and Luo, F. (2019) Dual Magnetic Behavior of Dysprosium(III) Molecular Magnet and Co(II) Spin-Crossover in an Isolated [3d]-[4f] Compound. *Inorganic Chemistry Communications*, **105**, 93-96. https://doi.org/10.1016/j.inoche.2019.04.030

[39] Yin, C., Hu, Z., Long, Q., Wang, H., Li, J., Song, Y., *et al*. (2019) Single Molecule Magnet Behaviors of Zn_4Ln_2 (Ln=Dy^{III}, Tb^{III}) Complexes with Multidentate Organic Ligands Formed by Absorption of CO_2 in Air through in Situ Reactions. *Dalton Transactions*, **48**, 512-522. https://doi.org/10.1039/c8dt03849j

[40] Fan, X., Yang, H., Li, D., Tian, H., Cao, F. and Dou, J. (2020) Three New Heterometallic Zn^{II}-Ln^{III} Complexes with a Windmill-Like Framework and Field-Induced SMM Behavior. *New Journal of Chemistry*, **44**, 2555-2560. https://doi.org/10.1039/c9nj05796j

[41] Liu, C., Hao, X. and Zhang, D. (2020) CO_2-Fixation into Carbonate Anions for the Construction of 3d-4f Cluster Complexes with Salen-Type Schiff Base Ligands: From Molecular Magnetic Refrigerants to Luminescent Single-Molecule Magnets. *Applied Organometallic Chemistry*, **34**, e5893. https://doi.org/10.1002/aoc.5893

[42] Liu, C., Hao, X. and Zhang, D. (2020) Effects of Substituents on Bridging Ligands on the Single-Molecule Magnet Properties of Zn_2Dy_2 Cluster Complexes. *Applied Organometallic Chemistry*, **35**, e6048. https://doi.org/10.1002/aoc.6048

[43] Liu, C., Zhang, D., Hao, X. and Zhu, D. (2020) Zn_2Ln_2 Complexes with Carbonate Bridges Formed by the Fixation of Carbon Dioxide in the Atmosphere: Single-Molecule Magnet Behaviour and Magnetocaloric Effect. *Dalton Transactions*, **49**, 2121-2128. https://doi.org/10.1039/c9dt04480a

[44] Wen, H., Hu, J., Yang, K., Zhang, J., Liu, S., Liao, J., *et al*. (2020) Family of Chiral Zn^{II}-Ln^{III} (Ln=Dy and Tb) Heterometallic Complexes Derived from the Amine-Phenol Ligand Showing Multifunctional Properties. *Inorganic Chemistry*, **59**, 2811-2824. https://doi.org/10.1021/acs.inorgchem.9b03164

[45] Zhu, S., Hu, J., Dong, L., Wen, H., Liu, S., Lu, Y., *et al*. (2020) Multifunctional Zn(II)-Yb(III) Complex Enantiomers

Showing Second-Harmonic Generation, Near-Infrared Luminescence, Single-Molecule Magnet Behaviour and Proton Conduction. *Journal of Materials Chemistry C*, **8**, 16032-16041. https://doi.org/10.1039/d0tc03687k

[46] Liu, C., Sun, R., Hao, X. and Wang, B. (2021) Chiral Co-Crystals of (s)-Or (r)-1,1′-Binaphthalene-2,2′-Diol and Zn_2Dy_2 Tetranuclear Complexes Behaving as Single-Molecule Magnets. *Crystal Growth & Design*, **21**, 4346-4353. https://doi.org/10.1021/acs.cgd.1c00246

[47] Wang, C.-M., Wu, Z., *et al*. (2021) The Zn_2Dy_2 Single-Molecule Magnet Constructed by Salen-Type Ligand and Hydroximic Acid. *Journal of Molecular Structure*, **1246**, Article 131231. https://doi.org/10.1016/j.molstruc.2021.131231

[48] Wang, H., Zhang, K., Wang, J., Hu, Z., Zhang, Z., Song, Y., *et al*. (2021) Influence of the Different Types of Auxiliary Noncarboxylate Organic Ligands on the Topologies and Magnetic Relaxation Behavior of Zn-Dy Heterometallic Single Molecule Magnets. *Inorganic Chemistry*, **60**, 9941-9955. https://doi.org/10.1021/acs.inorgchem.1c01217

[49] Panja, A., Jagličić, Z., Herchel, R., Brandão, P. and Jana, N.C. (2022) Influence of Bridging and Chelating Co-Ligands on the Distinct Single-Molecule Magnetic Behaviours in ZnDy Complexes. *New Journal of Chemistry*, **46**, 18751-18763. https://doi.org/10.1039/d2nj03793a

[50] Jing, Y., Wang, J., Kong, M., Wang, G., Zhang, Y. and Song, Y. (2023) Detailed Magnetic Properties and Theoretical Calculation in Ferromagnetic Coupling Dy^{III}-M^{II} 3d-4f Complexes Based on a 1,4,7,10-tetraazacyclododecane Derivative. *Inorganica Chimica Acta*, **546**, Article 121301. https://doi.org/10.1016/j.ica.2022.121301

[51] Li, G., Tang, H., Gao, R., Wang, Y., Sun, X. and Zhang, K. (2023) Tuning Quantum Tunneling in Isomorphic $\{M^{II}_2Dy^{III}_2\}$ "butterfly" System via 3d-4f Magnetic Interaction. *Crystal Growth & Design*, **23**, 1575-1580. https://doi.org/10.1021/acs.cgd.2c01198

[52] Roy, S., Du, J., Manohar, E.M., Aziz, T., Pal, T.K., Sun, L., *et al*. (2023) Syntheses, Structures, and Magnetic Properties of Novel [3 × 1 + 2 × 1] Pentanuclear Zinc(II)-Lanthanide(III) Cocrystal Complexes: Slow Magnetic Relaxation Behavior of the Dy(III) Analogue. *Crystal Growth & Design*, **23**, 2218-2230. https://doi.org/10.1021/acs.cgd.2c01256

[53] Wang, T., Yan, H., Che, Z. and Sun, W. (2023) Zn^{II}-Dy^{III} Single-Molecule Magnets Constructed by Salen-Type Ligand, Acetate and *B*-Diketonate. *Journal of Molecular Structure*, **1272**, Article 134179. https://doi.org/10.1016/j.molstruc.2022.134179

[54] Ding, Y., Han, T., Zhai, Y., Reta, D., Chilton, N.F., Winpenny, R.E.P., *et al*. (2020) A Study of Magnetic Relaxation in Dysprosium(III) Single-Molecule Magnets. *Chemistry—A European Journal*, **26**, 5893-5902. https://doi.org/10.1002/chem.202000646

[55] Konieczny, P., Czernia, D. and Kajiwara, T. (2022) Rotating Magnetocaloric Effect in Highly Anisotropic Tb^{III} and Dy^{III} Single Molecular Magnets. *Scientific Reports*, **12**, Article No. 16601. https://doi.org/10.1038/s41598-022-20893-2

[56] Watanabe, A., Yamashita, A., Nakano, M., Yamamura, T. and Kajiwara, T. (2011) Multi-Path Magnetic Relaxation of Mono-Dysprosium(III) Single-Molecule Magnet with Extremely High Barrier. *Chemistry—A European Journal*, **17**, 7428-7432. https://doi.org/10.1002/chem.201003538

[57] Konieczny, P., Pełka, R., *et al*. (2020) Relaxations in Mononuclear Tb^{3+} Single-Molecule Magnets. *The Journal of Physical Chemistry C*, **124**, 7930-7937. https://doi.org/10.1021/acs.jpcc.9b11057

[58] Eliseeva, S.V., Nguyen, T.N., Kampf, J.W., Trivedi, E.R., Pecoraro, V.L. and Petoud, S. (2022) Tuning the Photophysical Properties of Lanthanide(III)/Zinc(II) 'Encapsulated Sandwich' Metallacrowns Emitting in the Near-Infrared Range. *Chemical Science*, **13**, 2919-2931. https://doi.org/10.1039/d1sc06769a